# Non-protein activators of PAD4


Grzegorz P. Bereta[1], Ewa Bielecka[1], Karolina Marzec[1,2], Łukasz Pijanowski[1], Artur Biela[1,3], Piotr Wilk[1], Marta Kamińska[4], Jakub Nowak[1], Elżbieta Wątor[1], Przemysław Grudnik[1], Dominik Kowalczyk[2], Joanna Kozieł[2], Piotr Mydel[2,4], Marcin Poręba[5], **Tomasz Kantyka[1]***

***Affiliations:*** *[1]**Jagiellonian University, Malopolska Centre of Biotechnology; Krakow, Poland**. [2]Jagiellonian University, Department of Microbiology, Faculty of Biochemistry, Biophysics and Biotechnology; Krakow, Poland. [3]Jagiellonian University, SOLARIS National Synchrotron Radiation Centre; Krakow, Poland. [4]Broegelmann Research Laboratory, University of Bergen; Bergen, Norway. [5]Department of Chemical Biology and Bioimaging, Faculty of Chemistry, Wroclaw University of Science and Technology; Wroclaw, Poland.* ***Corresponding author. Email: tomasz.kantyka@uj.edu.pl**



**ABSTRACT**: Peptidylarginine deiminase 4 (PAD4) is citrullinating enzyme involvement in pathogenesis of rheumatoid arthritis. Activation of this enzyme by calcium remains unclear as calcium levels in the human body are typically too low for full activity. It has been proposed that allosteric activators of PAD4 improve calcium affinity of the enzyme. Several PAD4 activators have been identified recently, including optimized synthetic cyclic peptides or specific antibodies. They are rather results of iterative optimization or *in vitro* selection, not physiological molecules. Herein, we investigated the activation of PAD4 by glycosaminoglycans (GAGs) using heparin as model. We employed activity assays, chromatography, molecular interaction measurements (MST and SPR) and CryoEM to show activation of PAD4 and formation of PAD4-heparin complex. Our data show that PAD4 binds heparin, even at high salt concentrations. PAD4 is activated in the presence of heparin at sub-optimal concentrations of calcium and we observe that the activation mechanism depends on increasing PAD4 calcium affinity. We further demonstrate that activation by heparin depends on the length and charge of GAG molecule. Direct binding measurements using MST and SPR confirmed a tight interaction between PAD4 and heparin. CryoEM structures revealed PAD4 bound to heparin oligomers of varying lengths, showing different binding modes and supramolecular organizations of PAD4-heparin complexes. Mutagenesis studies indicated that PAD4 dimerization is essential for efficient activation. We demonstrate that cell surface binding of PAD4 depends on the GAG composition using CHO cell models and that heparin induces histone H3.1 citrullination and DNA release from human neutrophils. Additionally, other GAGs were identified as PAD4 activators. In summary, our findings present the first natural activators of PAD4, potentially explaining its role in physiological processes related to rheumatoid arthritis development.


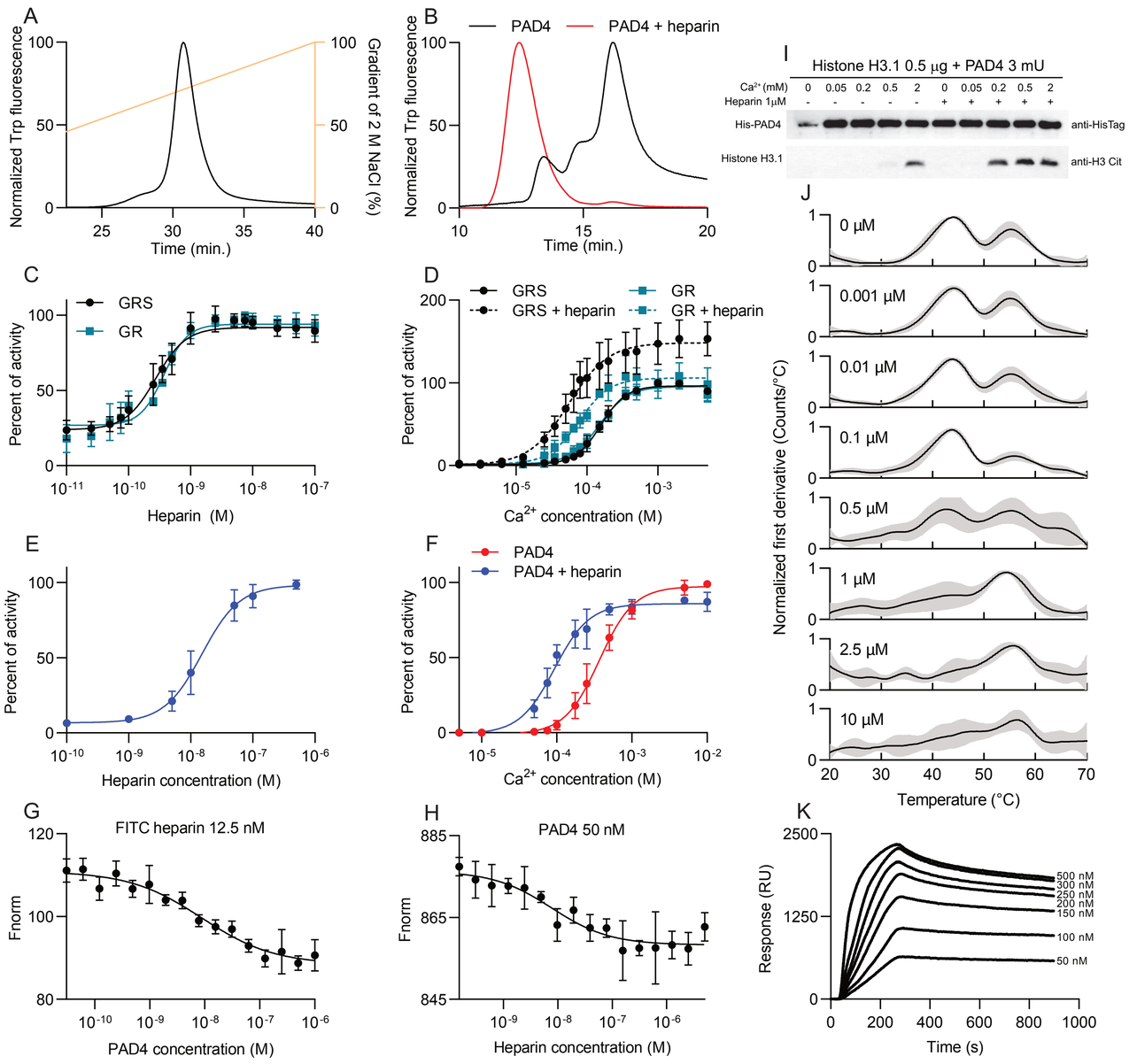


**Fig. 1. Binding and activation of PAD4 by heparin.** (**A**) Elution profile of PAD4 WT from a Poros heparin column in a salt gradient (**B**) Size exclusion chromatography of PAD4 on a Superdex 200 (**C**) PAD4 activity in sub-activatory $Ca^{2+}$ concentration (0.1 mM) with the addition of increasing heparin concentrations. $K_D$ = 0.27 ± 0.02 nM and 0.37 ± 0.03 nM for GRS and GR substrates, respectively. (**D**) Activity of PAD4 with/without addition of an activatory heparin concentration (1 μM) and increasing $Ca^{2+}$ concentrations. $Ca_{0.5}$ = GRS 155.8 ± 4.2 μM, GRS + heparin 55.1 ± 4.6 μM, GR 148.2 ± 6.4 μM, GR + heparin 77.4 ± 5.3 μM. (**E**) Activation of PAD4 by increasing concentrations of heparin in 0.1 mM $Ca^{2+}$. Apparent $K_D$ = 15.3 ± 1.4 nM. (**F**) Activation of PAD4 by $Ca^{2+}$ with and without 1 μM heparin. $Ca_{0.5}$ = no heparin 367 ± 13 μM, with heparin 92.9 ± 4.8 μM. (**G**) FITC-labelled heparin was at a constant concentration of 12.5 nM and PAD4 was titrated, in (**H**) PAD4 was kept at 50 nM and heparin was titrated. Hill equation was fitted and gave $K_D$ values of 8.8 ± 2.9 nM and 7.7 ± 4.5 nM for (**G**) and (**H**), respectively. (**I**) Western blot assay of PAD4 citrullination of human histone H3.1 at increasing $Ca^{2+}$ concentrations with or without 1 μM heparin. (**J**) Thermal unfolding curves of PAD4 with increasing heparin concentrations measured by nanoDSF. (**K**) SPR sensograms of increasing PAD4 concentrations with heparin immobilized on the chip surface. Binding was analyzed with one-site model with estimated $K_D$ 4.9 ± 1.1 nM.

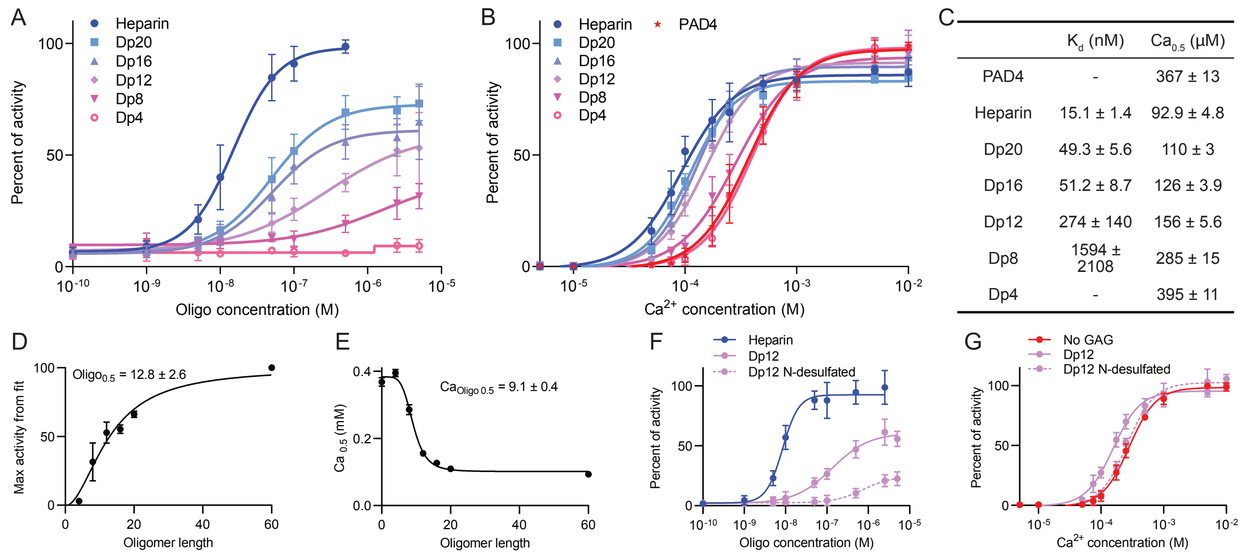


| | $K_d$ (nM) | $Ca_{0.5}$ (μM) |
|---|---|---|
| PAD4 | - | 367 ± 13 |
| Heparin | 15.1 ± 1.4 | 92.9 ± 4.8 |
| Dp20 | 49.3 ± 5.6 | 110 ± 3 |
| Dp16 | 51.2 ± 8.7 | 126 ± 3.9 |
| Dp12 | 274 ± 140 | 156 ± 5.6 |
| Dp8 | 1594 ± 2108 | 285 ± 15 |
| Dp4 | - | 395 ± 11 |

**Fig. 2. Effect of chain length and charge of heparin oligomers on the activation of PAD4.** (**A**) Activity of PAD4 in the presence of 0.1 mM $Ca^{2+}$ and heparin oligomers with decreasing length. (**B**) Activation of PAD4 by calcium in the presence of 1 μM heparin oligomers of different lengths. (**C**) Summary of apparent $K_D$ and $Ca_{0.5}$ values for heparin oligomers of various lengths from activity assays in (A) and (B). (**D** and **E**) maximum activity of PAD4 from fits in (A) and $Ca_{0.5}$ from (B) in the presence of heparin oligomers vs oligomer length. (**F**) PAD4 activity in 0.1 mM $Ca^{2+}$ and increasing concentrations of GAGs, Hill equation was fitted to obtain apparent $K_D$ values of 8.4 ± 0.6, 133 ± 23 and 741 ± 318 nM for heparin, Dp12, and Dp12 N-desulphated respectively. (**G**) Activation of PAD4 with $Ca^{2+}$ in the presence of 1 μM of GAGs, $Ca_{0.5}$ values from fitted Hill equation: 280.8 ± 7.5, 155.8 ± 5.3, 259.3 ± 9.5 μM for no GAG, Dp12 and Dp12 N-desulphated respectively.

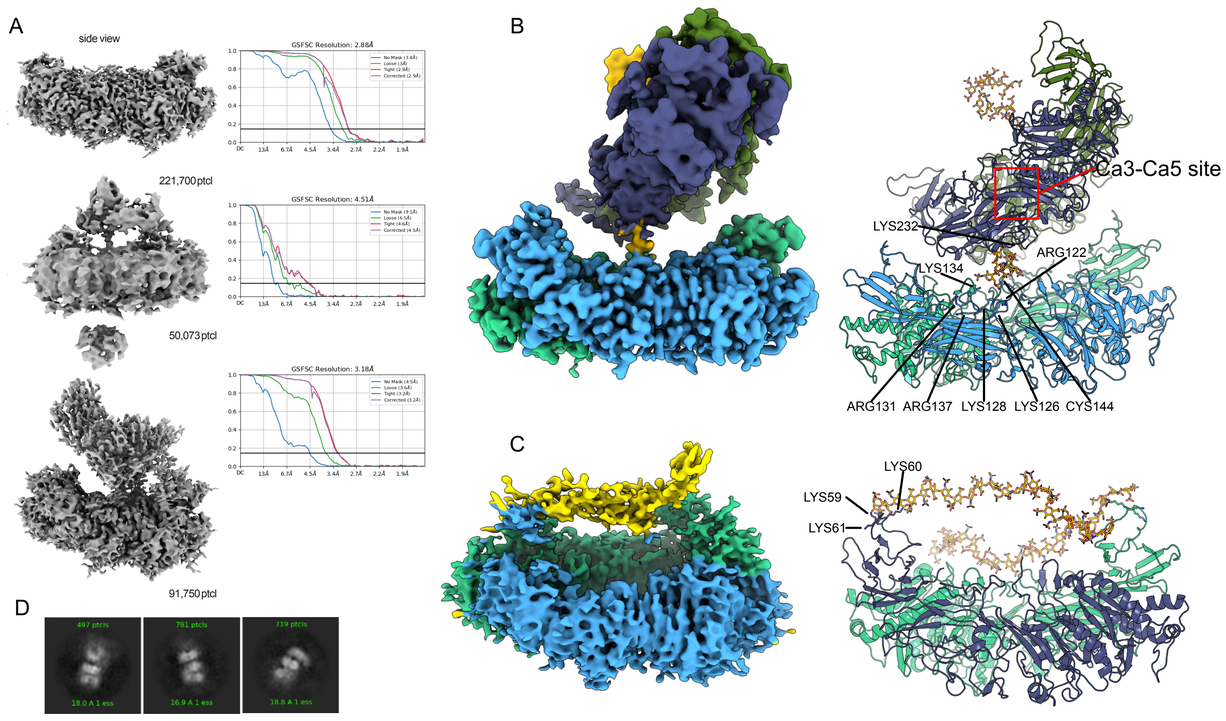


**Fig. 3. Structural organization of the PAD4-GAG complex.** (A) three main molecule classes were identified in the PAD4 sample incubated with dp20 heparin oligomer with corresponding CryoEM density maps. Structure solved in the presence of 0.1 mM $Ca^{2+}$(B) Optimized dimer-dimer structure in complex with dp12 oligomer. Interaction involves positive residues in the region Arg123 - Lys144 and Cys144 on the bottom dimer, while Lys232 and Ca3-Ca5 binding site are involved on dimer 2. Structure solved in the absence of $Ca^{2+}$. (C) Optimized single-dimer structure in complex with dp20 heparin oligomer. Interaction involves NLS Lys residues (Lys59-61). Structure solved in the absence of $Ca^{2+}$. (D) Some molecule classes from PAD4 - dp12 sample indicated formation of the longer chains of PAD4 dimers, as examplified by the triple dimer. Models are build based on the alpha-fold PAD4 structure. GAG chains indicate their approximate orientations.

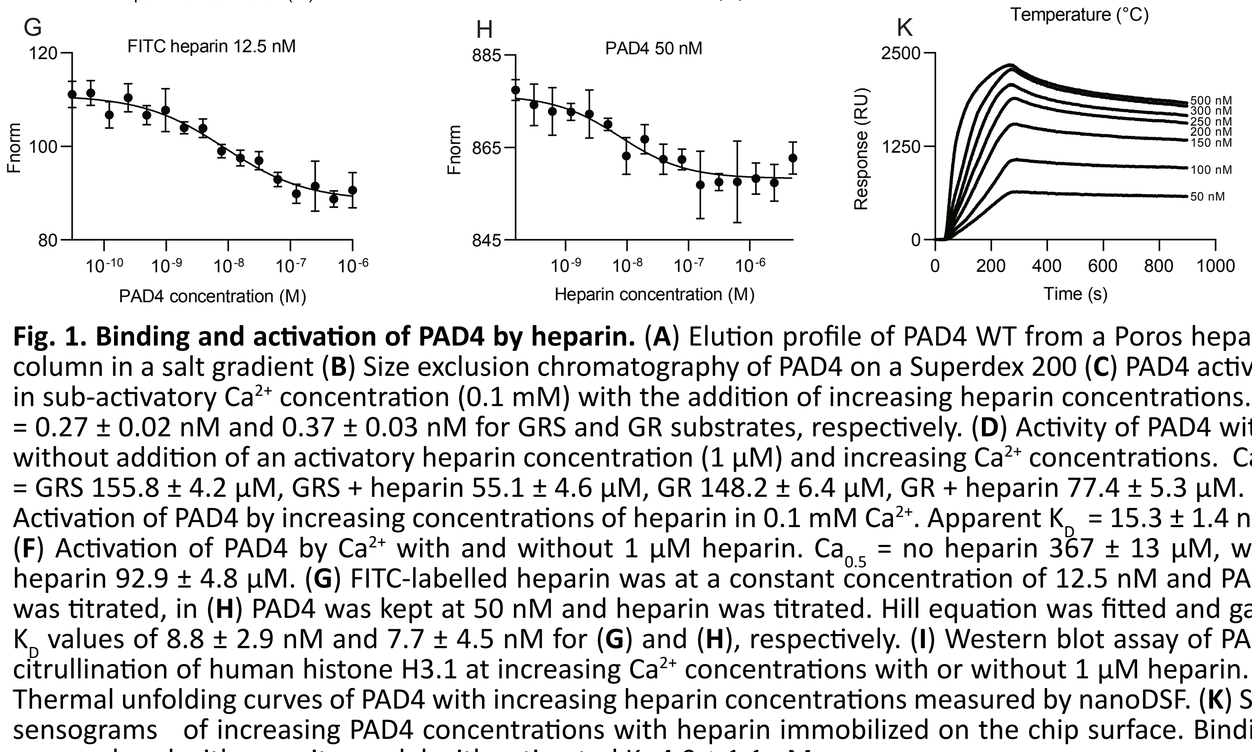


**Fig. 4. Biological properties of PAD4 activation with GAG.** (**A** and **B**) Activation of PAD4 in 0.1 mM $Ca^{2+}$ after the addition of 1 μM of GAG (DS- dermatan sulphate, HS – heparan sulphate, ChA – chondroitin A, ChC – chondroitin C, ChD – chondroitin D, Hep – heparin). (**A**) Colorimetric PAD4 activity assay with BAEE substrate. (**B**) Western blot assay of PAD4 citrullination of human histone H3.1. Blot against HisTag of PAD4 is presented as a control; results from representative experiment are shown. (**C**) FACS analysis of PAD4 binding to CHO-K1 wild type cells and its mutated cell lines with impaired GAG production (PgsB-650 and PgsA-745). Results are presented as signal fold change over background of cells not treated with PAD4 and normalized to control CHO cells. (**D**) Release of DNA from hPMN cells stimulated with increasing concentrations of heparin. Data is presented as mean ± SD, of signal normalized to time 0. (**E**) Immunocytochemistry staining of hPMNs stimulated with heparin for 4 hours at indicated concentrations. Blue – DNA, green – citrullinated histone H3, red – PAD4. Statistical significance was tested with one-way ANOVA;ns – not significant, * - $p < 0.05$, ** - $p < 0.01$, *** - $p < 0.001$, **** - $p < 0.0001$

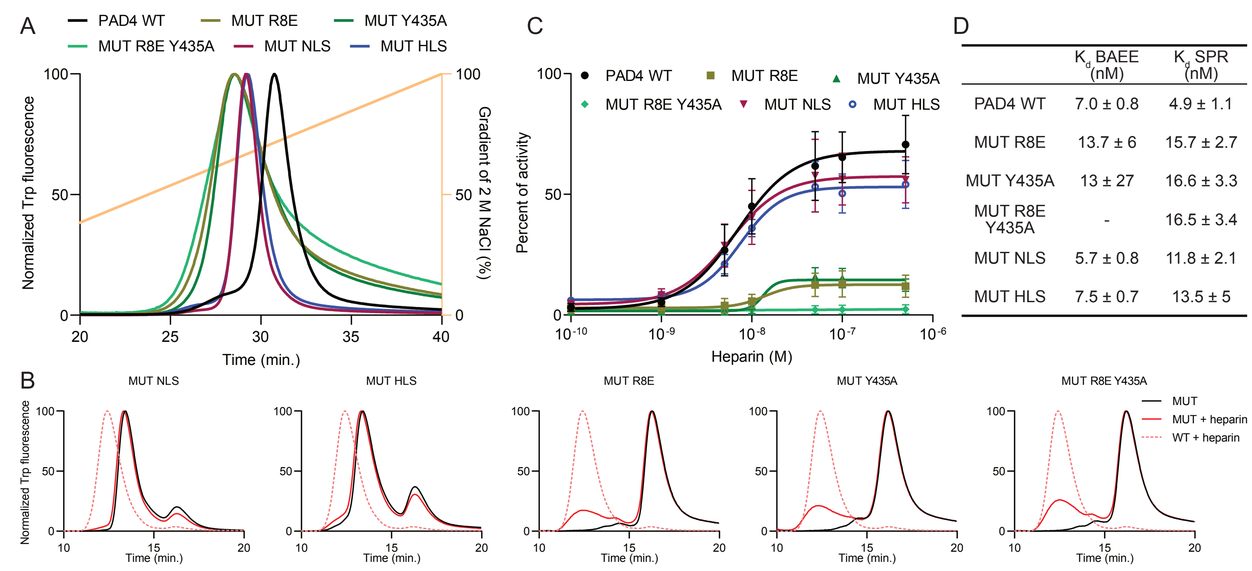


D

| | $K_d$ BAEE (nM) | $K_d$ SPR (nM) |
|---|---|---|
| PAD4 WT | 7.0 ± 0.8 | 4.9 ± 1.1 |
| MUT R8E | 13.7 ± 6 | 15.7 ± 2.7 |
| MUT Y435A | 13 ± 27 | 16.6 ± 3.3 |
| MUT R8E Y435A | - | 16.5 ± 3.4 |
| MUT NLS | 5.7 ± 0.8 | 11.8 ± 2.1 |
| MUT HLS | 7.5 ± 0.7 | 13.5 ± 5 |

**Fig. 5. Characterization of heparin binding to PAD4 dimerization mutants (R8E, Y435A, R8E Y435A) and regions involved in interaction with heparin (HLS: K126S K128S R131S K134S R137S and NLS: K59S K60S K61S K81S K91S).** (**A**) Elution profiles of PAD4 WT and mutants from a Poros heparin column (**B**) Size exclusion chromatography of PAD4 mutants with and without 5 μM heparin on a Superdex 200 column (**C**) Activation of PAD4 and mutants with heparin in 0.1 mM $Ca^{2+}$.Hill equation was fitted to calculate apparent $K_D$ for each mutant showed in (**D**) together with $K_D$ from SPR assay of interaction with immobilized heparin.


*Presented research was supported by Norway Financial Mechanism for years 2014 - 2021 under the GRIEG Project (2019/34/H/NZ1/00674) to Tomasz Kantyka, PhD.*